Electronic Supplementary Material (ESI) for Sustainable Energy & Fuels.

Electronic Supplementary Information

Harnessing Electrochemical pH Gradient for Direct Air Capture with Hydrogen and Oxygen By-Products in a Calcium-Based Loop

Congquan Zhou,[a,‡] Jihong Ni,[a,‡] Huiqi Chen,[a,‡] and Xiaofei Guan [a,*]

[a] School of Physical Science and Technology, ShanghaiTech University, 393 Huaxia Middle Road, Shanghai, 201210, China

‡ These authors contribute equally to this work.

* E-mail: guanxf@shanghaitech.edu.cn

Table of Contents:

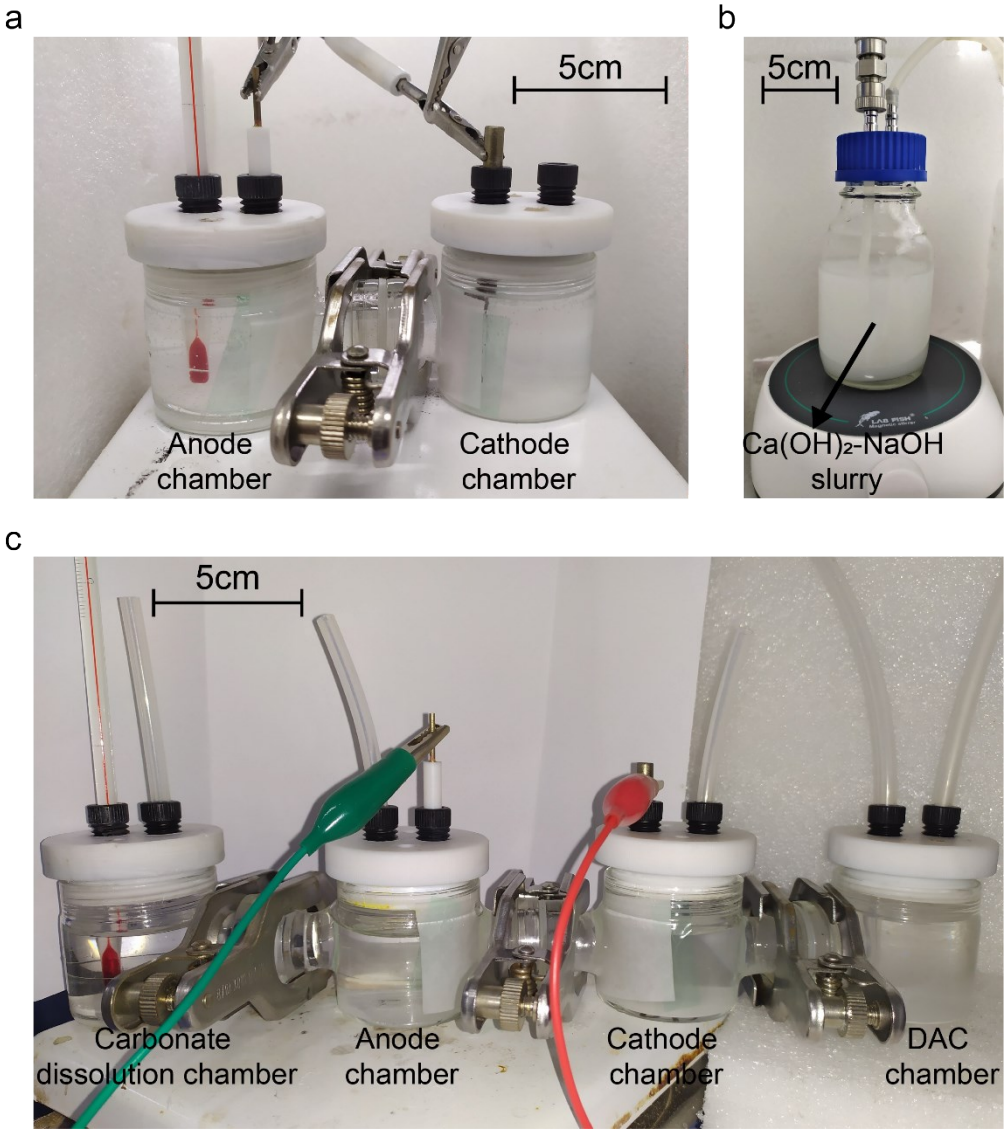

Fig. S1. Digital images of (a) the two-chamber H-cell for $CaCO_3$ dissolution and $Ca(OH)_2$ precipitation, (b) the single-chamber reactor for CO_2 capture in $Ca(OH)_2$-NaOH slurry, and (c) the four-chamber H-cell for simultaneous CO_2 capture and carbonate regeneration.

Note S1. Feasibility of TGA for quantitative analysis of $Ca(OH)_2$-$CaCO_3$ mixture:

The equilibrium composition for 1 kmol of $Ca(OH)_2$ and 1 kmol of $CaCO_3$ as a function of temperature is shown in Fig. S2a. $Ca(OH)_2$ starts to decompose at above 150 ℃ and the decomposition finishes at ~ 500℃. $CaCO_3$ starts to decompose at ~ 500 ℃ and finishes at ~ 1000℃. In practice, however, a constant flow of Ar removes the water vapor and carbon dioxide continuously and enable $Ca(OH)_2$ decomposition to start at ~ 340 ℃ and complete at ~ 420 ℃. In comparison, $CaCO_3$ decomposition starts at ~ 500 ℃ and completes at ~ 740 ℃. In a typical TGA test, $Ca(OH)_2$-$CaCO_3$ mixture samples exposed to an Ar environment (flow rate: 50 ml/min) were heated from room temperature to 200 ℃ at a rate of 10 ℃/min and held at 200 ℃ for 30 minutes to remove all the water vapor. The samples were then heated to 1000 ℃ at a rate of 4 ℃/min. The temperature profile and the relative weight decrease for the decomposition of a $Ca(OH)_2$-$CaCO_3$ mixture sample was shown in Fig. S2b. The two weight losses due to the decomposition of $Ca(OH)_2$ and $CaCO_3$, respectively, were observed with no overlaps. Therefore, a quantitative analysis of $Ca(OH)_2$-$CaCO_3$ mixture based on thermogravimetric result is feasible. It is noted that 1.84 wt.% $CaCO_3$ impurity existed in the as-received $Ca(OH)_2$, as determined by TGA, and was subtracted in calculations to obtain the exact amount of $CaCO_3$ formed during DAC.

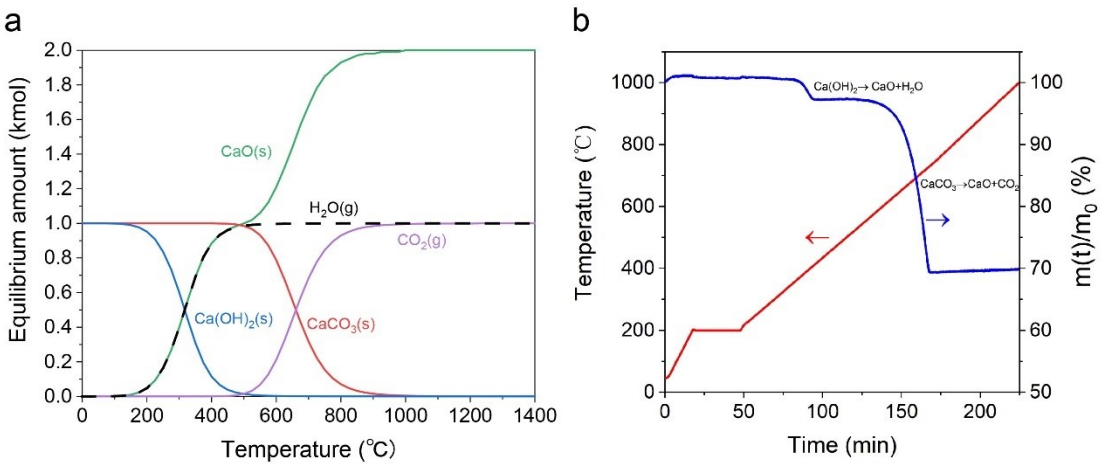

Fig. S2. (a) Equilibrium composition of $CaCO_3$ and $Ca(OH)_2$ vs. temperature at 1 bar. The starting amounts of both $CaCO_3$ and $Ca(OH)_2$ were set to 1 kmol for the thermodynamic calculation. (b) Temperature profile and relative weight decrease during a typical TGA run for quantitative analysis of a $Ca(OH)_2$-$CaCO_3$ mixture.

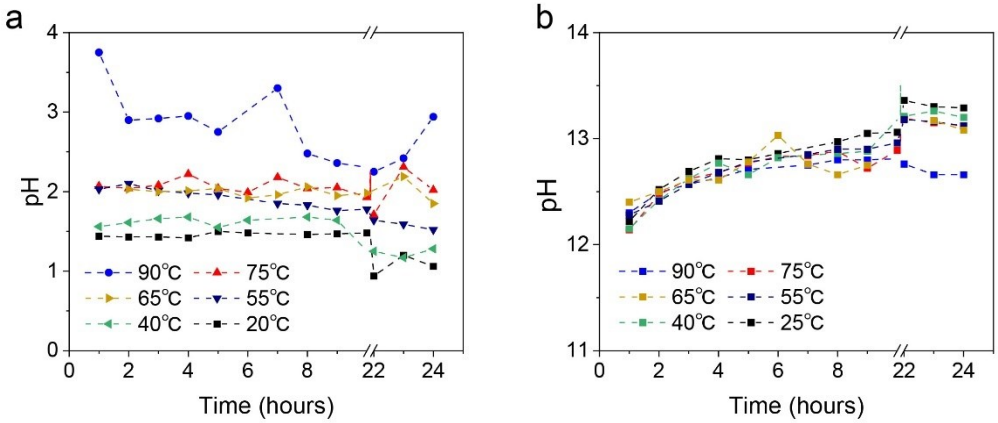

Fig. S3. The change of pH values of (a) anolytes (b) catholytes during electrolysis performed at different temperatures under an applied current of 40 mA for 24 hours.

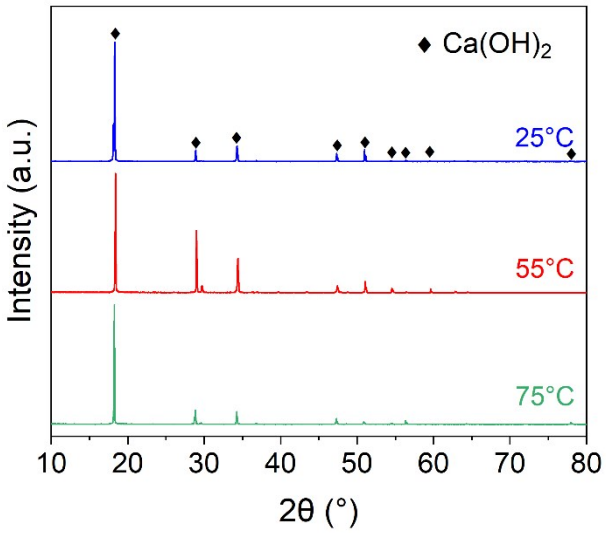

Fig. S4. Powder XRD patterns of the typical samples obtained from the precipitates collected in the cathode chambers after electrolysis experiments under 40 mA for 24 hours at 25, 55, 75℃, respectively. The data from the standard PDF card for $Ca(OH)_2$ (No. 00-044-1481) are used to index the diffraction peaks.

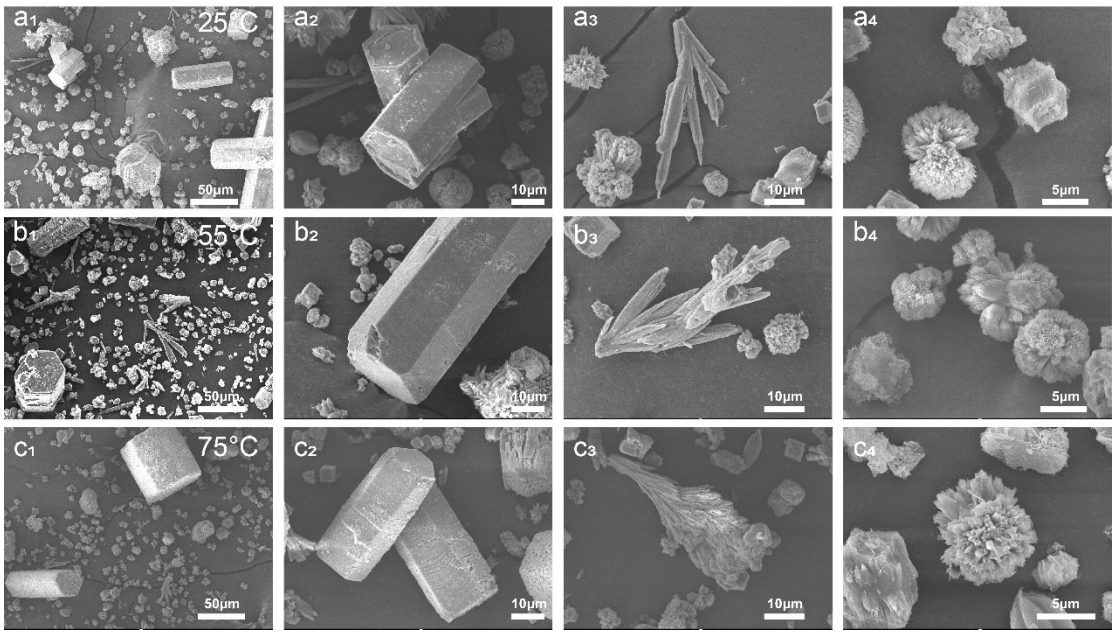

Fig. S5. SEM images of the $Ca(OH)_2$ precipitates collected from the cathode chamber after electrolysis experiments under 40 mA for 24 hours at (a_1-a_4) 25 ℃, (b_1-b_4) 55 ℃, and (c_1-c_4) 75 ℃, respectively.

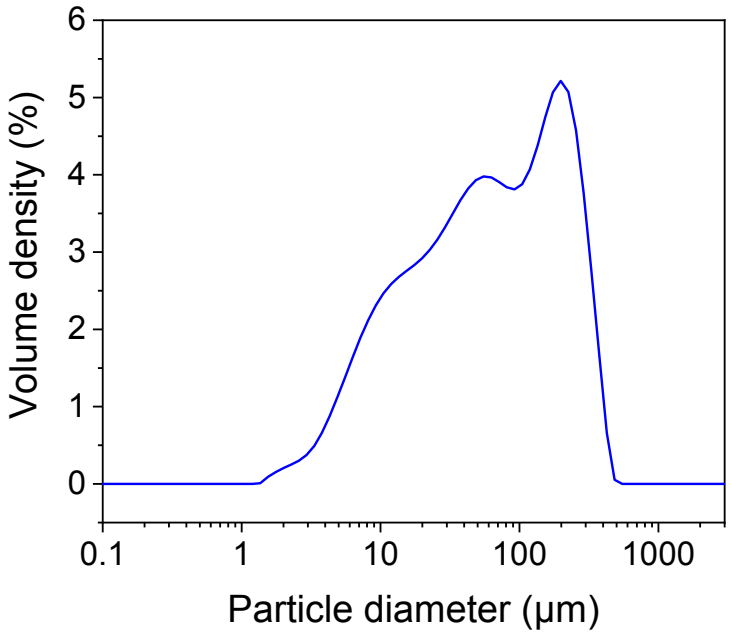

Fig. S6. The particle size distribution of the $Ca(OH)_2$ formed in the cathode chamber after electrolysis experiments under 40 mA for 24 hours at 75 ℃.

Note S2. Thermodynamic equilibrium composition of $Ca(OH)_2$–NaOH-air system:

Thermochemical equilibrium computations were carried out based on HSC chemistry database[1]. Consider a $Ca(OH)_2$–NaOH slurry bubbled with air containing 420 ppm of CO_2, the relationship between equilibrium amounts of species in the system and temperature is shown in Fig. S7. Thermodynamically speaking, the carbonation reactions of both $Ca(OH)_2$ and NaOH by CO_2 are favorable at ambient temperature with near 100% CO_2 capture.

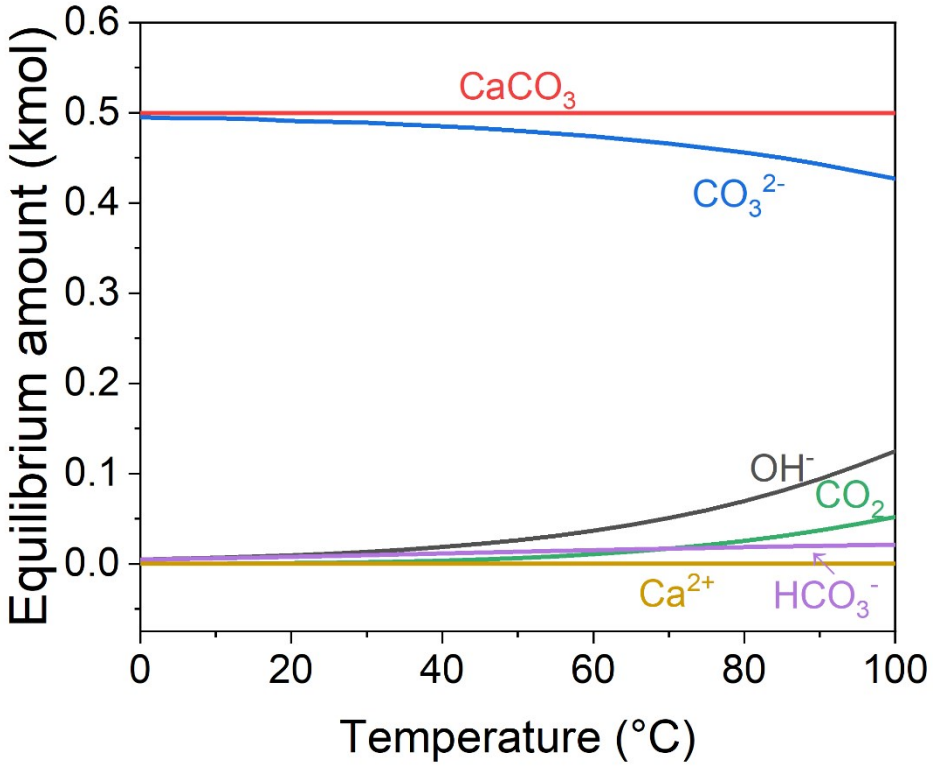

Fig. S7. The temperature dependence of equilibrium composition of products when $Ca(OH)_2$-NaOH slurry is exposed to air containing 420 ppm of CO_2 at 1 bar. Initial stoichiometry: 1 kmol Na^+ + 1 kmol OH^- + 0.5 kmol $Ca(OH)_2$ + 50 kmol H_2O + 1 kmol CO_2 + 500 kmol O_2 + 1880 kmol N_2.

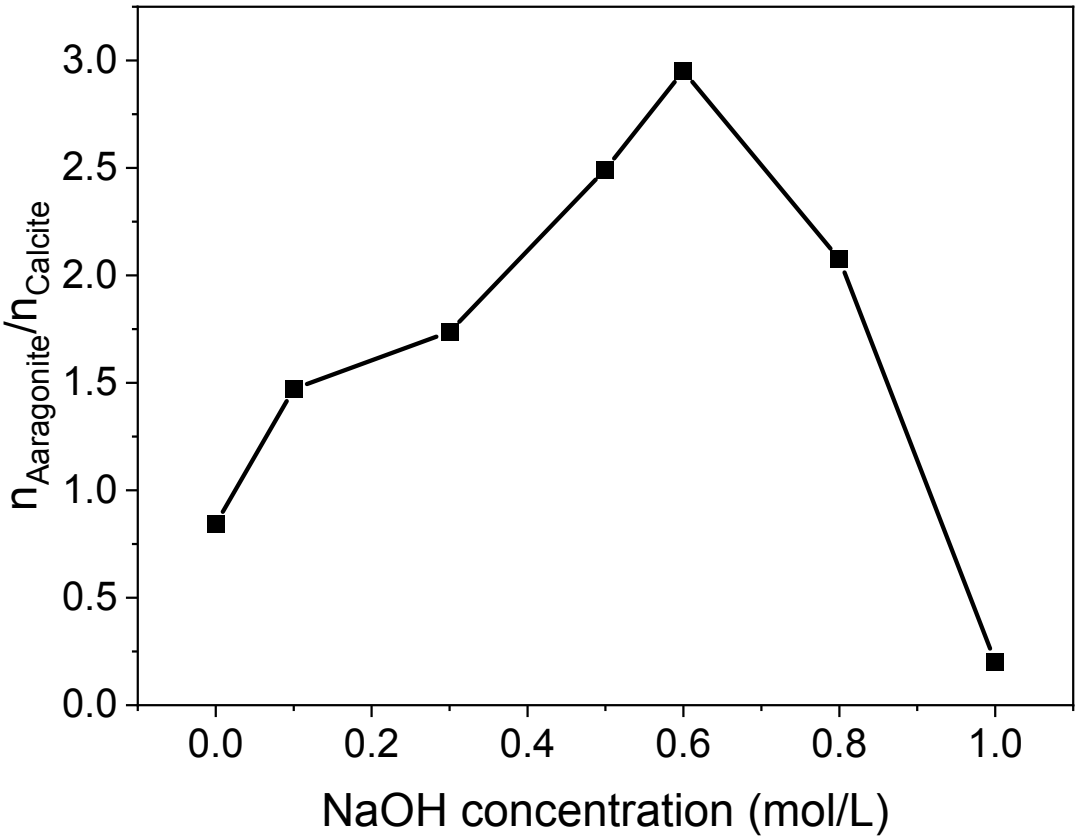

Fig. S8. The molar ratio of aragonite to calcite in the precipitates formed in $Ca(OH)_2$ slurries with different NaOH concentrations after 24-hour CO_2 absorption from air.

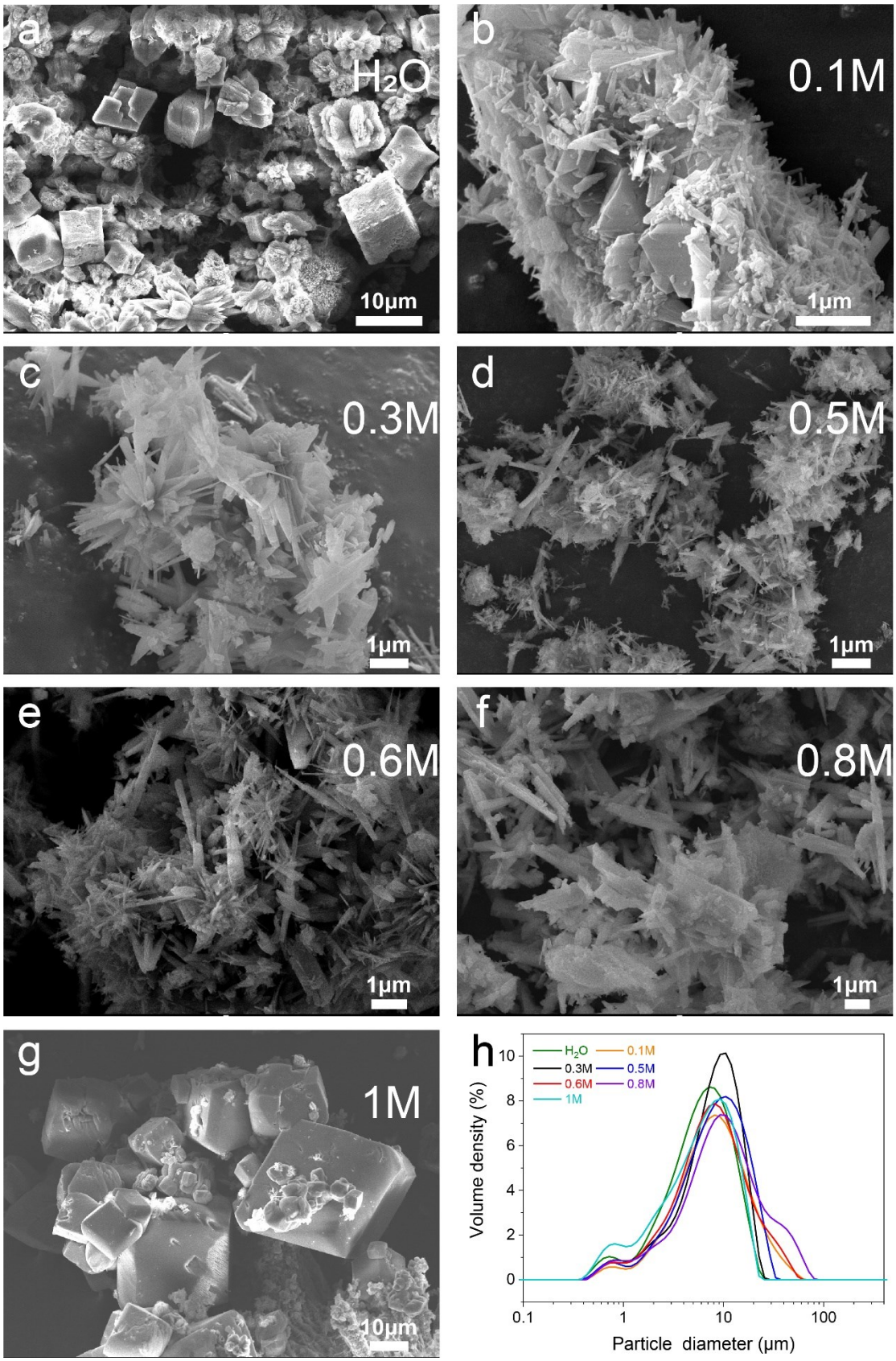

Fig. S9. SEM images and the particle size distribution of the precipitates collected after 24-hour CO_2 absorption in $Ca(OH)_2$ slurries of different NaOH concentrations.

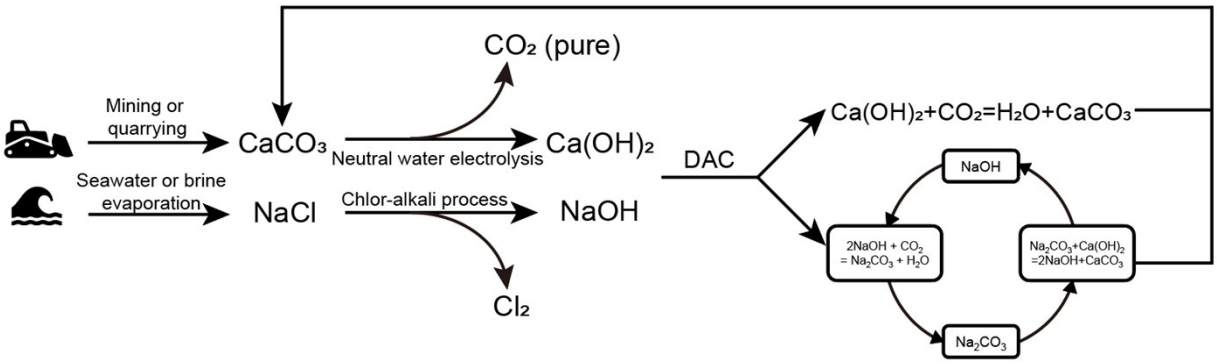

Fig. S10. Schematic representation of two-step direct air capture (DAC) process that takes account of the sources of $CaCO_3$ and NaOH. Dilute CO_2 is captured by $Ca(OH)_2$ slurry added with NaOH catalyst.

Note S3. Thermodynamic analysis for the necessity of pH gradient:

In aqueous solution, dissolved CO_2 (aq) can be converted to CO_3^{2-} through the following two reactions:

$$CO_2(aq) + H_2O \rightarrow HCO_3^- + H^+ \quad \text{(S1)}$$

$$HCO_3^- \rightarrow CO_3^{2-} + H^+ \quad \text{(S2)}$$

The equilibrium constants for reaction (S1) and (S2) are:[1]

$$K_{S1} = \frac{[H^+][HCO_3^-]}{[CO_2(aq)]} = 4.435 \times 10^{-7} \quad \text{(S3)}$$

$$K_{S2} = \frac{[CO_3^{2-}][H^+]}{[HCO_3^-]} = 4.676 \times 10^{-11} \quad \text{(S4)}$$

These equations can be solved and the relations between molar fractions (α) of different carbonic species and the $[H^+]$ are given as follows:

$$\alpha_{CO_2(aq)} = \frac{[H^+]^2}{[H^+]^2 + [H^+]K_{S1} + K_{S1}K_{S2}} \quad \text{(S5)}$$

$$\alpha_{HCO_3^-} = \frac{[H^+]K_{S1}}{[H^+]^2 + [H^+]K_{S1} + K_{S1}K_{S2}} \quad \text{(S6)}$$

$$\alpha_{CO_3^{2-}} = \frac{K_{S1}K_{S2}}{[H^+]^2 + [H^+]K_{S1} + K_{S1}K_{S2}} \quad \text{(S7)}$$

The CO_2 equilibrium diagram is plotted according to Eqs. S5-7, as shown in Fig. S11. The dominant dissolved carbonic species alters by changing the pH. CO_2 (aq) dominates at a pH below 4 while CO_3^{2-} is the predominant specie in the solution of which pH is above 12. Therefore, to realize a simultaneous CO_2 fixation in the absorption chamber and a CO_2 release in the anode chamber, a large pH gradient is necessary.

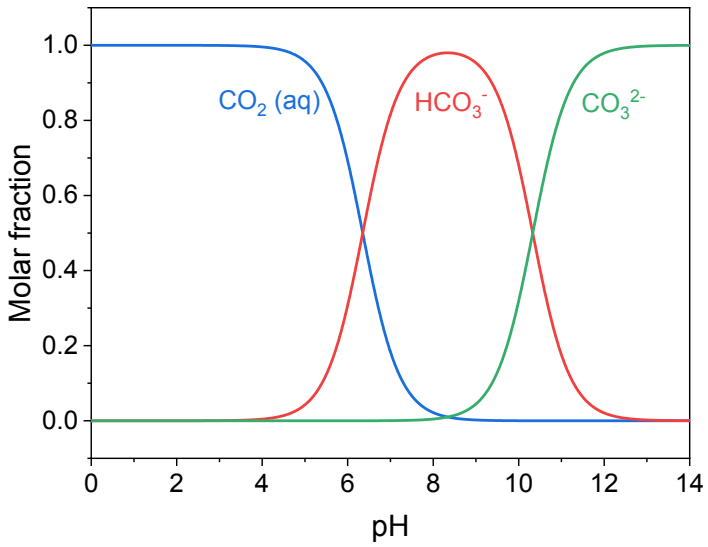

Fig. S11. Effect of pH on the CO_2 equilibrium in aqueous solution at 25 ℃.

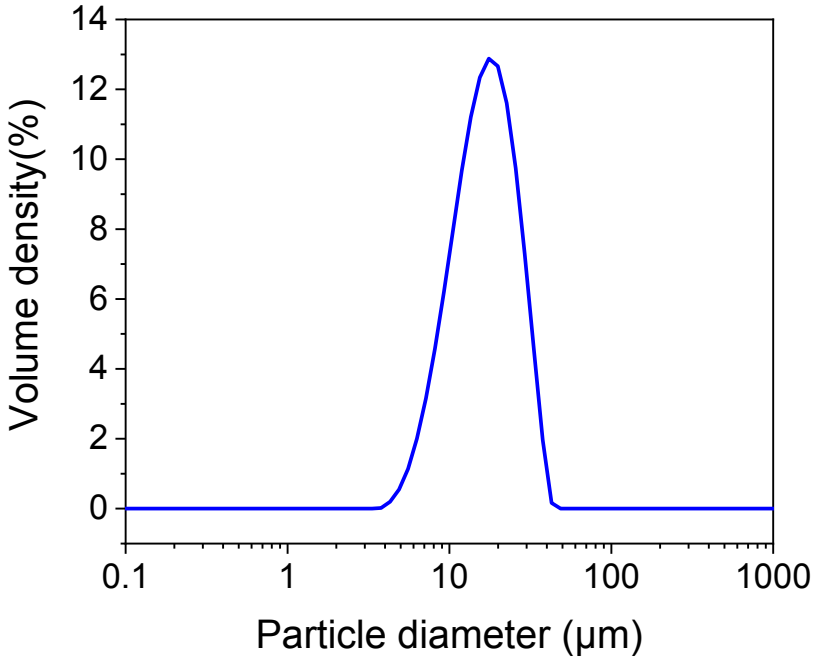

Fig. S12. The particle size distribution of the precipitates collected in the DAC chamber after 50-hour simultaneous direct air capture and carbonate regeneration.

Note S4. Nernst potential for water electrolysis:

As shown in the Pourbaix diagram for water (Fig. S13), the Nernst potential for water electrolysis is 1.205 V when the neutral electrolysis starts with an electrolyte of pH=6.57 at 55 ℃. With the progress of the electrolysis, the pH gradient between catholyte and anolyte contributes to an increase in the voltage for water splitting by 65.1×ΔpH (in mV). Therefore, when using a large pH gradient, the Nernst potential for water electrolysis increases (e.g. 1.72 V for pH=4 at anode and pH=12 at cathode).

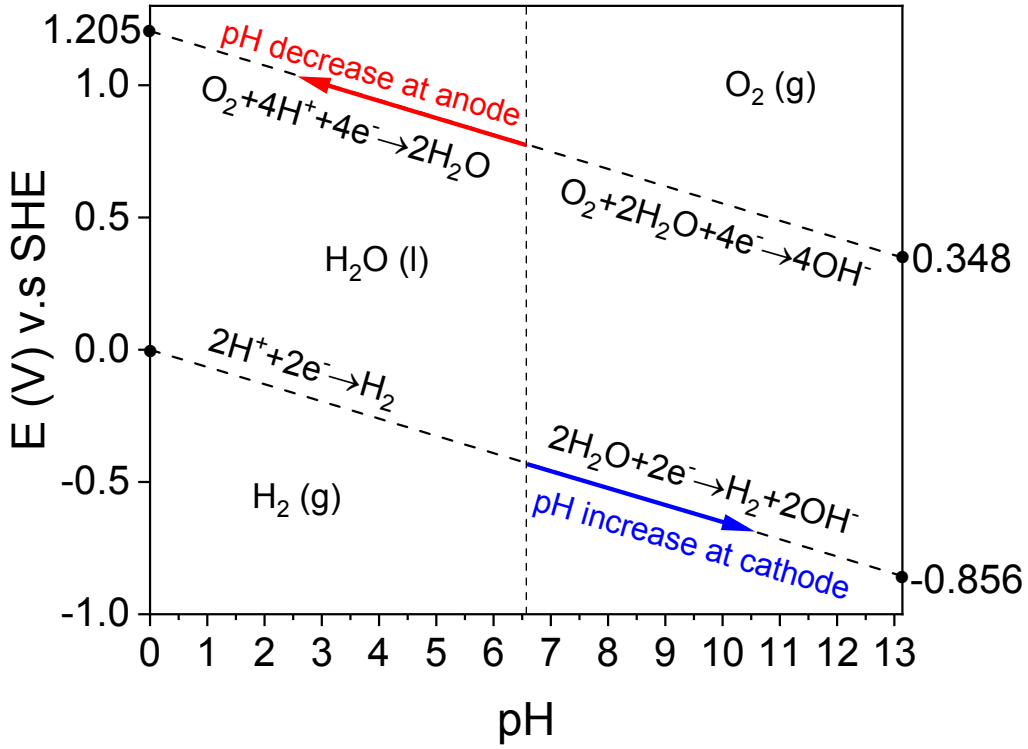

Fig. S13. Pourbaix diagram for water at 55 ℃.

Table S1. Material balance for the capture and release of 1 mol/s of CO_2 via the simultaneous DAC and sorbent regeneration process.

No.	Chambers		T (℃)	Mass flow rate (kg/h)	Reaction enthalpy change (kJ/mol CO_2)
1	Carbonate dissolution chamber	$CaCO_3$(s) in	55	360	
		CO_2(g) out		158.4	
		Reaction (5)			-15.875
2	Anode chamber	H_2O(l) in	55	64.8	
		O_2(g) out		57.6	
		Reaction (1)			284.880
3	Cathode chamber	H_2O(l) in	55	129.6	
		H_2(g) out		7.2	
		Reaction (2)			100.117
4	DAC chamber	air in	40	248571.4	
		CO_2-lean air out		248413.0	
		$CaCO_3$(s) out		360	
		Reaction (6)			-107.276
		Reaction (13)			17.449

Note S5. Material balance and energy efficiency:

The material balance for a scaled-up simultaneous CO_2 capture and sorbent regeneration is presented in Table S1, assuming a simultaneous capture of 1 mol/s of CO_2 and a regeneration of 1 mol/s $CaCO_3$. The operation temperatures of the chambers were identical to those described in the section on "demonstration of simultaneous direct air capture and carbonate regeneration". Further assumptions include: all the chambers operate isothermally; the evaporative loss of water during the operation is omitted; all the substances are pure; all the reactions achieve chemical equilibrium.

Solid $CaCO_3$ is added into the carbonate dissolution chamber at a rate of 360 kg/h, while 15.875 kJ/mol CO_2 of heat is released through the carbonate dissolution reaction (reaction 5). The unit kJ/mol CO_2 is equivalent to kW for a CO_2 capture rate of 1 mol/s. For water electrolysis in the anode and cathode chambers, splitting water at a rate of 194.4 kg/h requires 384.997 kW in total. In the DAC chamber, the capture of CO_2 by OH^- (reaction 6) rejects 107.276 kW as heat to the surrounding environment, part of which was offset by the endothermic association between Ca^{2+} and CO_3^{2-} (reaction 10) at 40 ℃.

It can be seen that the net reaction for the whole system capturing 1 mol CO_2 and regenerating 1 mol $CaCO_3$ simultaneously is written as follows with $\Delta G_{S8}{}^{55℃} = 397.412\ kJ/mol$.

$$3H_2O \rightarrow H_2 + 0.5O_2 + 2H^+ + 2OH^- \qquad \text{(S8)}$$

By combining with the actual energy expenditure observed in the section on "demonstration of simultaneous direct air capture and carbonate regeneration", the energy efficiency for a large-scale operation can be estimated. For an applied current of 40 mA, the mean voltage was 4.31 V during the operation. The CO_2 capture time is 48 hours and the fraction of CO_2 captured is set to be 0.9 to simplify the calculation. It is assumed that the temperatures of the reactors can be maintained by using the wasted heat from electricity generation supported by the promising development of heat-power cogeneration. Therefore, based on a lab-scale unoptimized system, the energy efficiency, defined as the ratio of the Gibbs free energy change of the net reaction to the actual energy expenditure per mole CO_2 captured,[2] for large-scale simultaneous CO_2 capture and $CaCO_3$ regeneration process is roughly estimated:

$$Energy\ efficiency = \frac{\Delta G_{S8}{}^{55℃}}{\frac{UIt}{n_{CO_2\ captured}}} = 15.1\%$$

References for ESI:

1. Roine, A. *HSC Chemistry Database 5.11*, HSC Chemistry Database 5.11, Outokumpu Research: Helsinki, Finland, 2002.

2. Rau, G. H.; Carroll, S. A.; Bourcier, W. L.; Singleton, M. J.; Smith, M. M.; Aines, R. D., Direct electrolytic dissolution of silicate minerals for air CO2 mitigation and carbon-negative H2 production. *Proc Natl Acad Sci USA* **2013,** *110* (25), 10095-100.